P1.1

HIGH-RESOLUTION MODELING ANALYSIS OF HAZARDOUS WINDS ASSOCIATED WITH MESOSCALE DISTURBANCES FOR THE SAFETY OF RAILWAY TRANSPORTATION SYSTEM IN A COASTAL AREA

Tetsuya Takemi*
Disaster Prevention Research Institute, Kyoto University, Uji, Kyoto, Japan

1. INTRODUCTION

The land of Japan is characterized by steep and complex terrain, which may influence the occurrence of extreme weather events such as torrential rain and damaging wind. Since the temporal and spatial variability of winds is very high, the effects of steep/complex terrains are particularly significant in inducing gusty winds. Thus, understanding not only flow structures associated with microscale meteorological phenomena but also terrain effects on wind variability is critically important for the prediction and mitigation of wind disaster. Such understanding should be of use in predicting wind environment as well as in assessing wind energy resources.

In addition, the recent development of mesoscale meteorological models enables one to simulate more accurately the local wind variability under realistically represented meteorological conditions, which lead to evaluating quantitatively the simulated wind fields against observational data in complex terrain (Jimenez et al. 2008; Rife and Davis 2005). Thus, representing steep/complex terrain in meteorological models with a high spatial resolution becomes more critical for quantitative wind forecasts.

In this study, we develop a high-resolution meteorological simulation system that incorporates 50-m mesh digital elevation map data to a mesoscale meteorological model, the Weather Research and Forecasting (WRF) Model. The numerical simulations are performed for high wind cases in a coastal area in order to diagnose the surface wind variability for the safety of railway transportation system. The analysis area chosen is the Shonai Plains, Yamagata Prefecture, Japan, where high wind events frequently occur during the passage of explosively developing extratropical cyclones in winter. The simulations are conducted for the cases in the 2007/2008 winter season. By conducting regional meteorological simulations that resolve small-scale terrain features, we discuss the representation of surface wind variability.

Corresponding author address:
Tetsuya Takemi, Disaster Prevention Research Institute, Kyoto University, Gokasho, Uji, Kyoto 611-0011, Japan; e-mail: takemi@storm.dpri.kyoto-u.ac.jp

2. MESOSCALE METEOROLOGICAL MODEL AND SIMULATION SETUP

2.1 *THE NUMERICAL MODEL AND TERRAIN DATA PROCESSING*

The mesoscale meteorological model used here is the Advanced Research Weather Research and Forecast Model (WRF/ARW, version 2.2.1) (Skamarock et al. 2005) which is developed by National Center for Atmospheric Research and other collaborators. This model solves a non-hydrostatic, compressible equation system for the atmosphere, discretized on the Arakawa-C staggered grid system. The third-order Runge-Kutta method is used for time differencing, and the fifth-order (third-order) upwind scheme is used for differencing horizontal (vertical) advection terms. The WRF model has a nesting capability that can resolve the area of interest with a fine grid spacing. In this study, four nested computational domains (with the top being at 50 hPa) are set, with the outermost domain (1780 km by 1460 km) covering the main island of Japan with a horizontal grid spacing of 8.1 km, decreasing the grid spacing by one third in each inner domain, and thereby the innermost domain (50 km by 38 km) covering the Shonai area and its surroundings with a 300-m grid. The vertical coordinate system is a terrain-following system based on the hydrostatic pressure which is normalized by the pressures at the surface and the upper boundary. The number of vertical grids is 40, with 10 grids in the lowest 500 m. The time step for the outermost domain is 45 sec, and that for the innermost domain is 0.56 sec.

In determining the initial and boundary conditions, we use the 6-hourly Mesoscale Analysis data (MANAL) of Japan Meteorological Agency (JMA), the 6-hourly Final Analysis data of National Center for Environmental Prediction, and the daily Merged Sea Surface Temperature

(MGDSST) analysis of JMA. The horizontal resolutions of MANAL and MGDSST are 10 km and 0.25 degree, respectively, which are useful for high-resolution regional simulations. Six-hourly SST data are made by interpolating in time the daily MGDSST analyses. These 6-hourly data are provided as the boundary conditions at the lower and the lateral boundaries of the outermost domain as well as the initial condition for the outermost domain.

For creating the terrain and land-use/land-cover (LU/LC) data for the simulation, the three outer domains use the global 30-second topography data (GTOPO30) from the U.S. Geological Survey (USGS). On the other hand, the 50-m mesh digital elevation dataset by the Geographical Survey Institute of Japan (GSI50) is used for creating the terrain in the innermost domain. The computational grid spacing for the innermost domain is 300 m, and a 16-point averaging is performed for the original GSI50 terrain, thus the model terrain being created. The land/sea mask for this domain is re-defined with the GSI50 terrain. However, because the GSI50 does not include LU/LC information, these data for the innermost domain are interpolated from the USGS 24-category Global LU/LC data.

These terrain and meteorological data processing routines are incorporated into the WRF Preprocessing System (WPS). The model terrains and the initial and boundary conditions for the WRF simulations are created by this preprocessing system. Figure 1 shows the model area and terrain for the innermost computational domain.

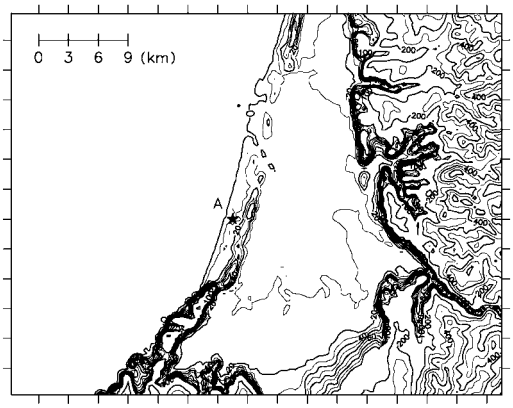

Figure 1: The model terrain for the innermost computational domain.

2.2 *SIMULATION SETUP*

In order to represent meteorological settings as accurately as possible within a given computational resource, several options for parameterizing cloud microphysics, cumulus convection (only for the outermost domain), atmospheric radiation, surface energy transfer, and planetary-boundary-layer (PBL) mixing were determined. Among these parameterizations, PBL mixing is the most important for simulating surface wind fields; this study chose a Mellor-Yamada Level 2.5 (MYJ) scheme (Janjic 1990). This scheme, formulated based on a Reynolds-averaging approach, solves a prognostic equation for turbulent kinetic energy (TKE) that determines the vertical-component eddy viscosity coefficients with a diagnostic equation of length scale. The mixing is done locally between the adjacent grid levels. In this scheme, the horizontal-component eddy viscosity coefficients are determined by the intensity of local horizontal wind shear and the horizontal grid spacing.

For comparison, a non-local mixing (YSU) scheme (Hong et al. 2006) was also examined; the result, however, showed that the YSU scheme gave a smoothed variation of wind speed and was not able to represent short-term temporal variation as in the MYJ scheme. Overall, it was found that the YSU scheme did not produce better accuracy than the MYJ scheme. Although there is a significant sensitivity of PBL simulations to mixing parameterization (Berg and Zhong 2005), it should be noted that the recent study by Weisman et al. (2008) has shown that this non-local scheme induces excessive mixing and hence more enhanced convection. Therefore, the MYJ scheme is regarded as a baseline PBL scheme here.

The other issue concerning the PBL scheme is the choice of the vertical grid spacing and distribution. Of course, a higher resolution is desirable; however, the number of grids is limited by a computational resource. Historically, in numerical weather prediction community the efforts have been mainly devoted to increasing the horizontal grid resolution. To the author's knowledge, there is no consensus on how to set the vertical grid spacing and distribution specifically in the PBL for a particular choice of PBL scheme. This issue in relation to the PBL scheme should be extensively investigated for various meteorological settings in a future study.

2.3 *SIMULATED CASES*

For the present simulations, we choose high wind events over the analysis area during the 2007/2008 winter season from the data obtained by the surface weather observation network implemented for the railway weather research

Table 1 List of selected high wind cases during the 2007/2008 winter season for the numerical simulations. Maximum Instantaneous wind speed and wind direction at the same time at the Sakata weather station in the Shonai Plains are summarized.

Month	Day	Wind Speed (m/s)	Wind Direction	Month	Day	Wind Speed (m/s)	Wind Direction
10	20	24.1	WSW	1	13	23.4	NW
11	15	20.0	WSW	1	17	20.5	WNW
11	18	27.0	WNW	1	24	26.9	WSW
11	19	25.6	WNW	1	25	20.2	NW
11	20	24.8	WSW	2	13	23.5	WNW
11	21	24.0	NW	2	14	22.8	W
11	22	29.5	W	2	20	18.9	W
12	5	18.8	W	2	23	27.3	NW
12	30	18.7	WNW	2	24	27.7	WNW
12	31	24.8	WNW	2	28	20.9	WNW
1	1	20.8	WNW	3	1	21.3	WNW
1	9	23.7	W				

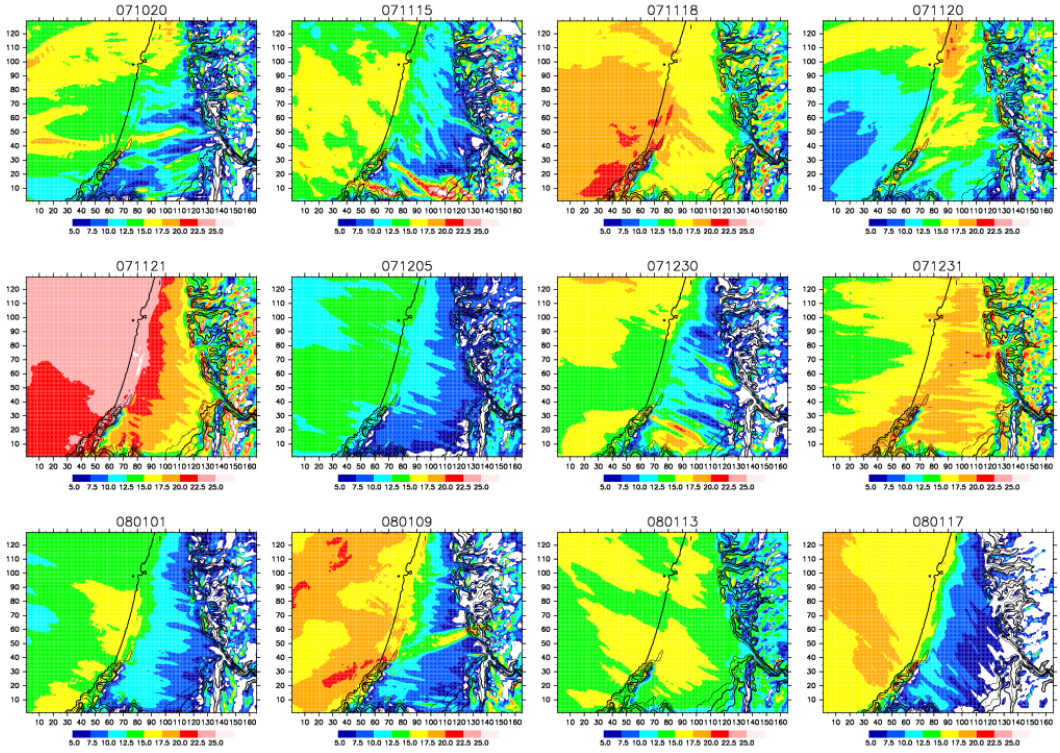

Figure 2: Map of standard deviation normalized by mean wind speed (in %) from the time series of wind speed at each grid location for the cases listed in Table 1.

project (Kusunoki et al. 2008). High wind events are defined as those having sudden increase in wind speed over 10 m/s at a short period of time (i.e., one minute) during October 2007 and March 2008. The selected cases are listed in Table 1, which indicates the maximum instantaneous wind speed on each selected day at the Sakata weather station in the Shonai Plains, Yamagata, Japan.

The numerical simulations with the 300-m grid spacing are performed for all the cases listed in Table 1. The simulated periods for each case

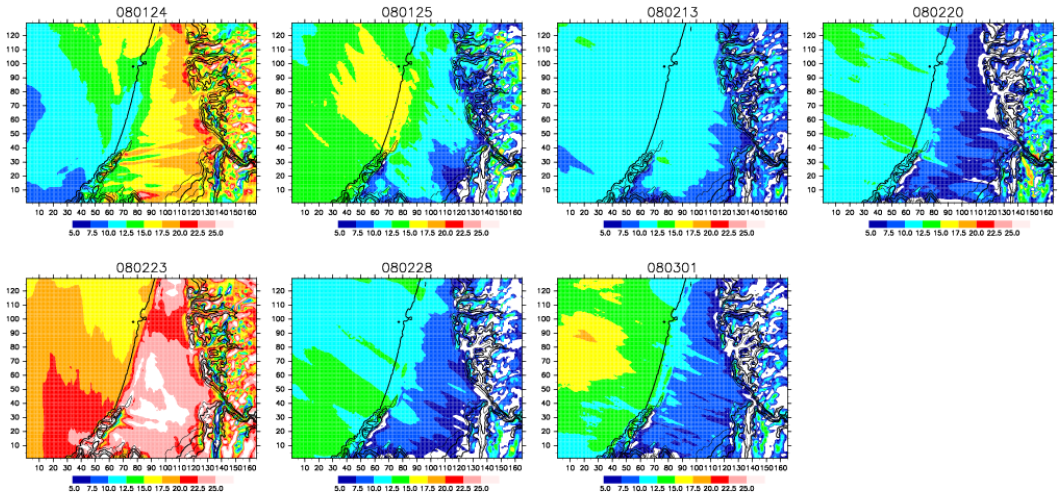

Figure 2: (*continued*)

range from 12 to 48 hours, with 6-18 hour simulations for the innermost domain, depending on the cases.

The simulated results for the innermost domain are stored at every 1-min interval and are used for the present analyses.

3. RESULTS

Figure 2 shows the horizontal distribution of wind speed standard deviation divided by mean from the time series outputs at each grid point for the cases listed in Table 1. The variability for this map seems to be quite large depending on the cases: in one case the standard deviation is larger over the sea than over the land; while in another case the standard deviation is more significant over the land than over the sea.

It appears that there are hardly organized features among the simulated cases. However, by examining meteorological settings for each case, it is seen that mesoscale convective disturbances play a role in inducing high variability over the sea, while cold-air outbreak after the passage of cold front plays a role in inducing high variability over the land.

Figure 3 show the maps of mean and maximum wind speed for all the simulated periods. The strongest mean wind speeds are seen over the sea surface, since the roughness length at the sea surface (0.01 cm) is much smaller than that of land surface (tens of cm). Strong wind region extends from the sea surface into the Shonai Plains, gradually decreasing inland. There is a weak wind area in the southern end of the plains, which is located in the downstream of a steep terrain. In addition, the areas of strong winds are found at the foot of and within the eastern mountains; this again is due to the better representation of the terrain. The standard deviation map indicates a higher variability in the northern half of the plains and also near the steep slopes. The higher variability in the northern plains is due to the geographical feature of the plain, which is open to the west to northwest directions and is hence susceptible to strong winds without the deceleration by land-surface roughness. In other words, the small-scale linear-shaped hill has an impact on the surface wind field, despite that the height of the hill top is at most 50 m.

Figure 3 also exhibits the map of maximum wind speed at every grid point during the simulated period of the innermost domain. Areas of high maximum wind speed appear to penetrate inland from the gaps of and overriding the small, linear hill. Enhanced maximum wind speeds are specifically seen in the downstream of the gap (in the northern half of the plains) and also in the downstream of the hill (in the middle and the south of the plains). This indicates that the linear-shaped hill, in spite of its small scale, affects the development of and controls the location of the maximum wind speed at the surface. The map further suggests that the locations of strong winds would be nearly the same from case to case; this type of information should be of help for diagnosing the locations that are susceptible to wind disaster.

We have examined the turbulence intensity diagnosed in terms of the parameterized TKE computed in the MYJ scheme. The pattern of this distribution looks similar with that seen in Fig. 3. The most significant difference from that shown in Fig. 3 is the value over the sea surface; significant values of TKE are found over land surface, specifically where the effects of terrain play a role. This is clearly due to the difference in roughness between sea and land surfaces. This result suggests that the parameterized TKE

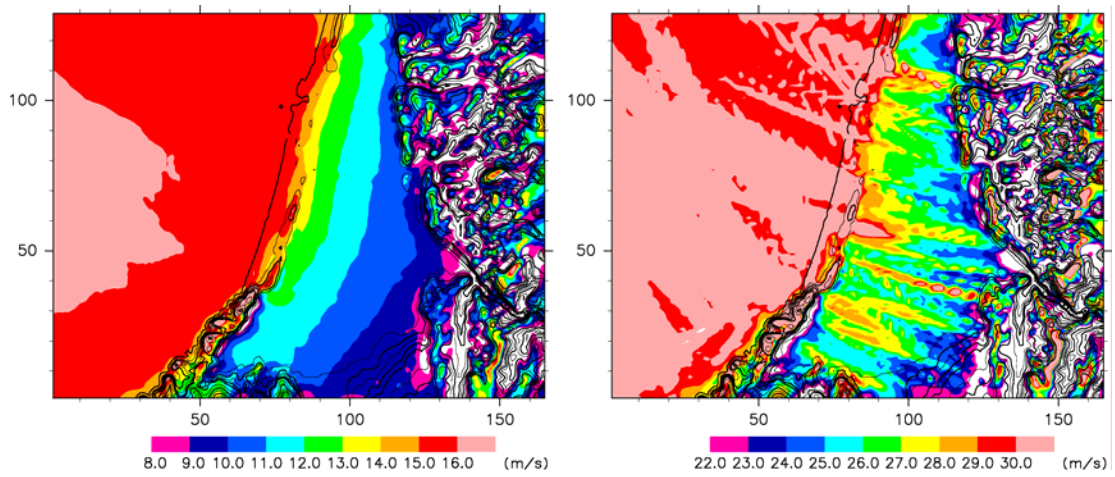

Figure 3: Map of mean wind speed (left) and maximum wind speed (right) from all the time series outputs for all the simulated cases.

primarily reflects the roughness and steepness of the surface terrain; the effects inherent in meteorological disturbances seem to play a secondary role in the specific case examined in this study.

The parameterized TKE seems to be a good measure in diagnosing the variation of strong winds in steep and complex terrains. The effects of TKE on wind variation were further examined by converting the TKE values to a velocity scale, by taking square root of twice the TKE value. Examining the horizontal distribution of the ratio of the TKE-velocity to the total wind speed in the analysis domain, the percentage significantly changed horizontally, which seems to closely correspond to surface elevations and terrain features. In addition, the distribution also depends on the land-use characterization (i.e., surface roughness length). Over the Shonai Plains, a gradual decrease inland of this percentage was able to be identified, despite that the surface for the area was characterized all by agriculture and had a roughness length of 15 cm. This suggests that the variability becomes the largest at the edge of the rougher surface. These characteristics of the TKE temporal and spatial variability indicate that higher TKE values well correspond to stronger wind speeds at the surface. The result further suggests that the parameterized TKE values from the MYJ scheme can be used for diagnosing surface strong winds resulted from terrain effects.

4. SUMMARY

We have developed a high-resolution meteorological simulation system that incorporates the 50-m mesh digital elevation map dataset of Japanese Geographical Survey Institute. This system is applied for a strong wind event over the Shonai Plains, Yamagata Prefecture, which locally induced a significant disaster. The simulation using this 50-m mesh dataset benefits from more accurate representation of terrain features than the case using a coarser-mesh terrain dataset (e.g., GTOPO30). The high-resolution simulation with the 300-m grid spacing can represent short-term and small-scale variability of surface winds that are primarily affected by surface roughness and topography. Even small-scale terrains such as low-topped linear-shaped hill seen in the west of the Shonai Plains have a significant impact on the variability of surface wind speed. One may argue that the 300-m grid spacing is not sufficient to closely mimic the topography from the 50-m mesh elevation data.

Maximum wind speeds at each grid location during the simulation period distribute inhomogeneously over the Plains. In addition, the parameterized TKE values obtained from the turbulence-closure scheme can be used for diagnosing surface strong winds that are mainly resulted from surface roughness and terrain, not from meteorological disturbances. However, the velocity scales converted from the TKE values account for at most 20 % of the total wind speeds over the Shonai Plains; the percentage seems to be much short of gust factors typically observed during high-wind events. Therefore, some other approach in addition to diagnosing TKE should be developed in order to realistically estimate gust factors under various meteorological and geographical conditions. Higher-resolution simulations that can explicitly resolve turbulent eddies should be conducted for this purpose in a future study.

There is an on-going research project on the observation, diagnosis, and forecasting of severe winds over the Shonai area (Kusunoki et al. 2008), which employs a dense surface observation network as well as Doppler radar observation. The dataset should be of use for high-resolution simulations. In addition to the representation of small-scale terrain in the high-resolution simulations, resolving small-scale structures embedded in meteorological disturbances are also important. The 300-m mesh simulation was able to reproduce a realistic microscale vortex structure on the order of 100 m, which spawned locally high winds over the Shonai Plains on 2 December 2007 (Inoue et al. 2009). A higher-resolution simulation with 120-m grid spacing is currently undertaken for the same case, which can capture a finer feature of the vortex disturbance and reproduce surface high winds. Resolving small-scales of both topography and meteorological disturbance in high-resolution simulations is vital for the analysis and forecasting of severe local winds.

5. ACKNOWLEDGMENTS

This study was supported by a grant (2007-02) from the Program for Promoting Fundamental Transport Technology Research from the Japan Railway Construction, Transport and Technology Agency. Kenichi Kusunoki at Meteorological Research Institute (MRI), who is the principle investigator of the project, is acknowledged for his help in conducting the present study. Toshiaki Imai, Takaaki Fukuhara (at Railway Technical Research Institute), Kotaro Bessho, Masahisa Nakazato, Shunsuke Hoshino, Wataru Mashiko, Shugo Hayashi, and Hanako Inoue (at MRI) are acknowledged for their efforts in choosing extreme wind events from the data obtained by the surface observation network over the Shonai Plains. The computation times were provided by the SuperComputer Laboratory, Institute for Chemical Research, Kyoto University.

6. REFERENCES

Berg, L. K., and S. Zhong, 2005: Sensitivity of MM5-simulated boundary layer characteristics to turbulence parameterizations, *J. Appl. Meteor*. **44**, 1467-1483.

Hong, S., Y. Noh, and J. Dudhia, 2006: A new vertical diffusion package with an explicit treatment of entrainment processes, *Mon. Wea. Rev.*, **134**, 2318-2341.

Inoue, H. et al., 2009: Fine-scale Doppler radar observation of a tornado and low-level misocyclones within a winter storm in the Japan Sea coastal region, *Mon. Wea. Rev*., submitted.

Janjic, Z. I., 1990: The step-mountain coordinate: physical package, *Mon. Wea. Rev*., **118**, 1429-1443.

Jimenez, P. A., J. F. Gonzalez-Rouco, J. P. Montavez, J. Navarro, E. Garcia-Bustamante, and F. Valero, 2008: Surface wind regionalization in complex terrain, *J. Appl. Meteor. Clim*., **47**, 308-325.

Kusunoki, K., et al., 2008: The Shonai Area Railroad Weather Project: Scientific objectives and experimental design, *Proc. 13th Conf. on Aviation, Range and Aerospace Meteorology*, New Orleans, LA, 20-24 January 2008, Amer. Meteor. Soc., P2.16.

Rife, D. L., and C. A. Davis, 2005: Verification of temporal variations in mesoscale numerical wind forecasts, *Mon. Wea. Rev.*, **133**, 3368-3381.

Skamarock, W. C., J. B. Klemp, J. Dudhia, D. Gill, D. M. Barker, W. Wang, and J. G. Powers, 2005: A description of the Advanced Research WRF Version 2, *NCAR/TN-468+STR*, 88 pp

Weisman, M., C. Davis, W. Wang, K. Manning, and J. B. Klemp, 2008: Experiences with 0-36-h explicit convective forecasts with the WRF-ARW model, *Wea. Forecasting*, **23**, 407-437.